Pergamon

Tetrahedron: *Asymmetry* 11 (2000) 2695–2704

TETRAHEDRON: *ASYMMETRY*

# Quantitative chirality of helicenes

Omer Katzenelson, Joseph Edelstein and David Avnir*

*Institute of Chemistry and The Lise Meitner Minerva Center for Computational Quantum Chemistry, The Hebrew University of Jerusalem, Jerusalem 91904, Israel*

Received 25 April 2000; accepted 13 June 2000

**Abstract**

Quantitative evaluation of geometrical chirality through the use of the Continuous Chirality Measure is employed to unveil correlations between chirality and several properties of helicenes. These include the efficiency of their chiral-chromatographic racemate separation, their optical rotation, their racemization energy and the melting points of the enantiomer-crystals. The non-monotonic behavior of the chirality of helicenes is shown to reflect the behavior of a theoretical helix. © 2000 Published by Elsevier Science Ltd.

## 1. Background

We continue to explore the consequences of treating chirality as a structural property to which a scale and degree can be attached,[1,2] concentrating on the series of helicenes. Several quantitative correlations between chirality and chemical, biochemical and physical parameters have already been identified, and these could have been, in fact, revealed only through the treatment of chirality as a quantitative structural property. Two recent examples are the correlations between the degree of chirality of fullerenes and the energetics of their enantiomerization;[3a] and the correlation between the degree of chirality of enzyme-inhibitors and their inhibition efficiency.[3b] The methodology we have been using, the Continuous Chirality Measure (CCM),[1,2] is an integral part of a more general approach of treating symmetry (any point group) as a continuous structural property.[4] The rationale, the approach, the practical solutions and the applications of chirality measurement with the Continuous Chirality Measure (CCM) methodology were described repeatedly in many of our previous papers.[1–4] Reviews,[5] other uses of the CCM approach and its modifications,[6] including an investigation of helicenes,[6a] and other methods to evaluate chirality[7] have been published. Here we recall briefly that the measure, $S(G)$, evaluates the minimal distance that the vertices of a size-normalized structure have to be translated in order to acquire achirality, where $G$ is the nearest achiral symmetry point group. In many cases, and for

* Corresponding author. E-mail: david@chem.ch.huji.ac.il

0957-4166/00/$ - see front matter © 2000 Published by Elsevier Science Ltd.
PII: S0957-4166(00)00235-4

all of the helicenes described below, the nearest achiral shape is of the point-group symmetry of $\{E,\sigma\}$, i.e. achirality due to a reflection plane, and so the chirality measure (strictly, in fact, the achirality measure) is $S(\sigma)$. We also recall here that $S(\sigma)=0$ means that the shape is achiral, and that as the structure becomes more chiral, $S(\sigma)$ increases (up to a maximum of 100, obtained for some cases of the more general Continuous Symmetry Measure methodology).[8] The chirality measure is a global shape parameter, and is therefore distinctly different from the characterization of helical structures through specific geometric features, such as has been the practice in the study of polypeptides.[9]

Here we correlate the quantitative chirality of helicenes with several of their properties. Thus, we re-analyse the results of the pioneering studies of Gil-Av[10] who resolved helicene (Fig. 1a) racemates using high-performance liquid chromatography. (*R*)-(–)- and (*S*)-(+)-2-(2,4,5,7-tetranitro-9-fluorenylideneaminoxy)propanoic acid (TAPA) were used as chiral charge–transfer complex-formation stationery phases by coating silica microparticles, and with it, the series of [6]-helicene to [14]-helicene racemates were completely resolved.[11] The enantioselectivity of this column—in terms of the resolution factors, *r*—towards the various helicenes, is shown in Fig. 2 and it reveals a rather complex trend: for the lower helicenes, *r* increases with size, then it passes through a maximum in [9]-helicene and increases again for the higher helicenes. (Since *r* values are the ratios between the capacity factors of the two enantiomers,[12] a similar trend (not shown here) is obtained by plotting the capacity factors of each enantiomer series as a function of size.) Interestingly, the optical rotations[12] of the helicenes follow a similar trend (Fig. 3) to the one observed for enantioselectivity: an increase in rotation up to a maximum, again at [9]-helicene, a decrease, and then a second increase up to [14]-helicene, with [11]-helicene deviating between the two figures. Can quantitative chirality relate to this behavior and reproduce it? A positive answer is presented below, along with other correlations found between the chirality of the helicenes and their racemization energy and between the chirality and melting points.

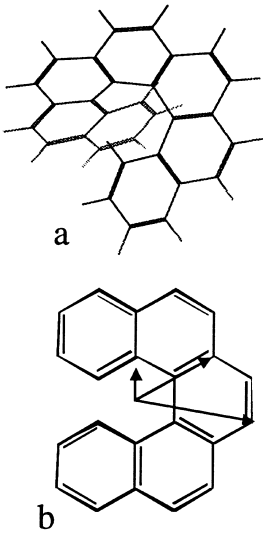


Figure 1. (a) (M)-[7]-Helicene, one of the carbohelicenes analysed in this study. We used the M–P handedness conversion, referring to left–right helices, respectively; (b) various radii used in this study, shown for [5]-helicene: inner (smallest), middle and outer (1.5 Å, 2.9 Å and 3.75 Å, respectively)

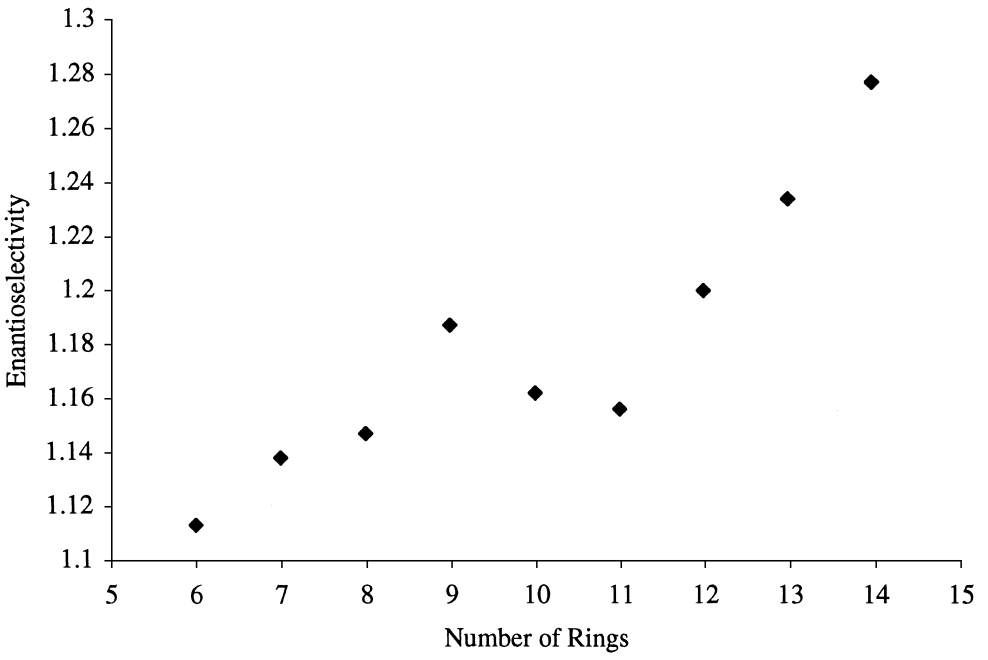


Figure 2. The enantioselectivity (resolution *r*-factor) of a chiral TAPA column towards helicenes as a function of their number of rings (after Gil-Av et al.)[10]

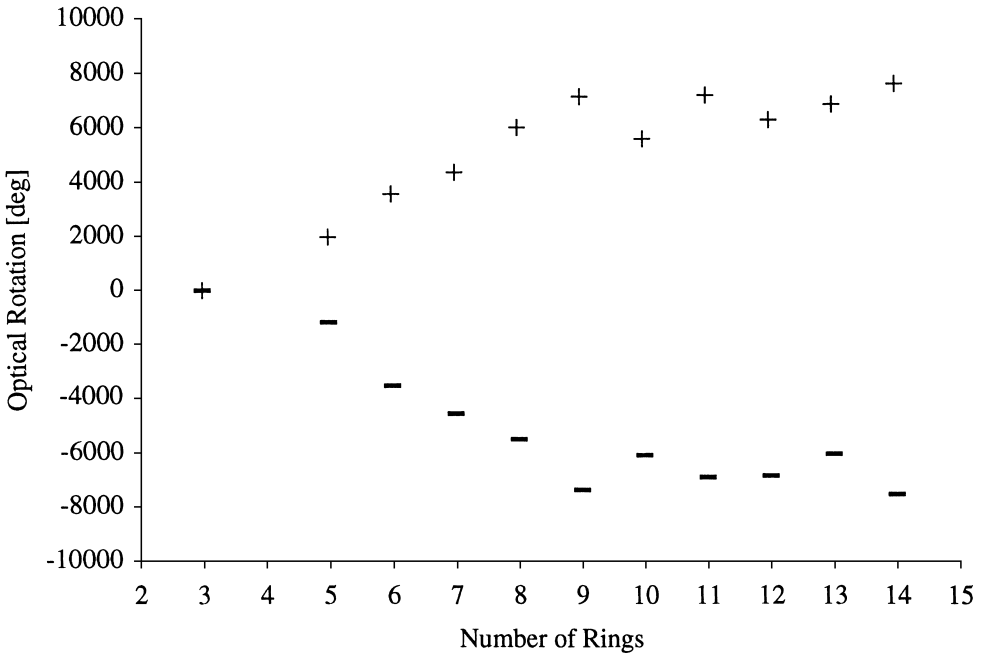


Figure 3. Optical rotation of helicenes as a function of the number of rings. (–) M, (+) P

## 2. Computational details

X-Ray crystallographic data is available for [3]–[7]-, [10]- and [11]-helicenes.[13] In order to obtain the structures of the full series of [3]–[19]-helicenes, the most stable structures were calculated using the Austin Method One (AM1) with Spartan.[14] The agreement between the experimental data and the calculated structures is good: only small rms deviations were found: 0.05 Å and 0.18 Å for [5]-helicene and [7]-helicene, respectively. The point-group symmetry of the helicenes was found to be $C_2$, as expected. Theoretical helices were constructed from a dense lace of points, as described in Section 3. Chirality values were calculated[1] from:

$$S_G = \frac{100}{nD^2} \sum_{i=1}^{n} (p_i - \hat{p}_i)^2 \tag{1}$$

where $n$ is the number of points which construct the helix, $p_i$, is their location, $\hat{p}_i$ is the corresponding point in the nearest, searched achiral configuration[15] and $D$ is a size normalization factor (the distance from the center of mass of the helix to the farthest vertex).

## 3. Results and analyses

### 3.1. The geometrical chirality content of helicenes and helixes

Plotting the geometrical chirality content of the helicenes versus their size (Fig. 4) reveals a remarkable resemblance to Figs. 2 and 3: chirality increases, passes through a first maximum at

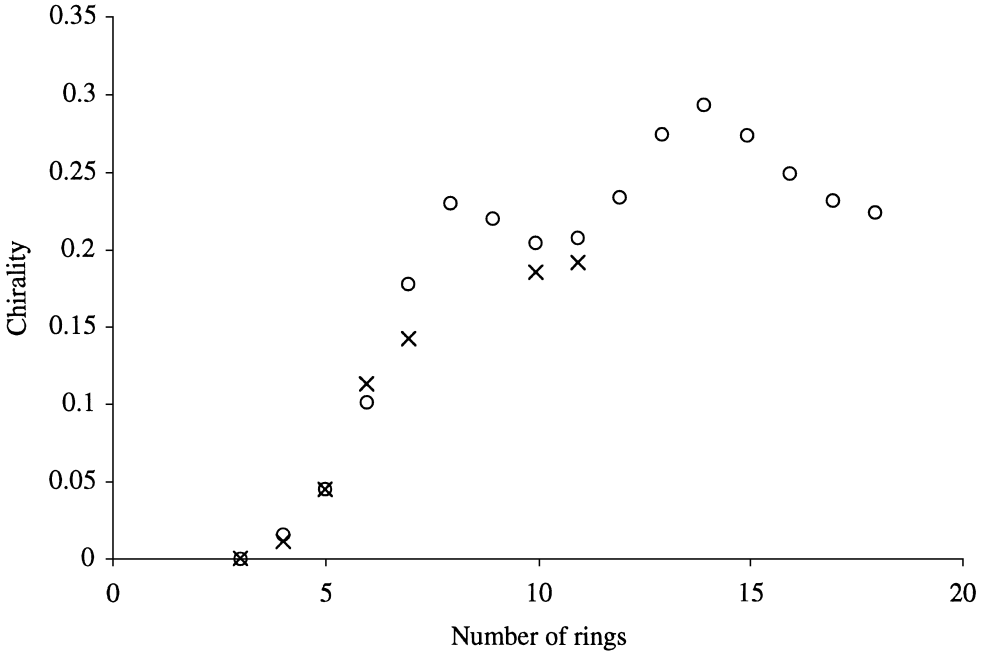


Figure 4. Chirality of helicenes as a function of the number of rings. (O) AM1 structures; (X) X-ray structures

[8]-helicene, and then through a higher one at [14]-helicene. The maximum at [8] is slightly shifted between the plots ([8] versus [9], respectively) and we relate to it below. We also show below that the maximum for [14]-helicene is global: [14]-helicene is the most chiral helicene.

In order to understand the behavior of Fig. 4, we now analyze the chirality of a general helix. Helix vertices are represented by the following four parameters: the radius ($r$), the number of turns ($n$), the pitch ($p$) and the density of points ($d$, i.e. the number of points along one turn):

$$\begin{cases} x_n = r \times \cos(n \times d) \\ y_n = r \times \sin(n \times d) \\ z_n = n \times p \end{cases} \tag{2}$$

Fig. 5a shows the chirality map of a helix (see figure caption for the specific parameters), how chirality changes as a function of the number of turns and the pitch. As clearly seen the ridge along the highest chirality value oscillates, and a cross-section at a typical helicene pitch shows it as well (Fig. 5b). The general feature seen in this figure is of a chirality function that passes through global chirality maximum value, and on this trend, are superimposed several maxima. Furthermore, for $r = 2.9$, maxima at the equivalent helix lengths of the [8]-, [9]- and [14]-helicene rings are retrieved. Let us first explain why the chirality value must pass through a maximum: for a very small number of points the helix has the shape of a small arch, barely expressing the helicity, and the chirality is consequently small. In fact, for the first three points in our helix presentation, this value is zero (and likewise it is zero for [2]-helicene (naphthalene) and practically zero for [3]-helicene (phenanthrene)). For a very large number of points, i.e. for an infinitely large number of turns all squeezed into the normalized unit length, the helix has the shape of a rod for which the turns are stacked nearly parallel: the helix at this extreme end is achiral again, i.e. has a chirality value of zero. Thus, the function which begins and ends at a zero value, must pass through some (maximal) non-zero value; as seen, this value is reached quite fast, i.e. after just 14/6 turns. The oscillatory character of the helix chirality values is due to the superposition of the oscillatory character of the helix, with the first peak after 8/6–9/6 rounds.

### 3.2. Property–chirality correlations

It is now clear that the physical and chirality behavior of the helicenes, as seen in Figs. 2–4, reflects directly, as should have been the case, the behavior of a simple helix. Slight shifts in the position of the first local maximum depend on which of the representative radii of the helicene (Fig. 1b) is taken. Thus enantioselectivity, which is determined mainly by the outer regions of the molecular shape, indeed showed (Fig. 2) a maximum at the [9]-helicene, reflecting the chirality of the outer rim. Optical rotation, due to the whole of the molecule, is best presented by the middle radius chirality, leading again to a maximum in [9]-helicene (Fig. 3). Geometrical chirality as a function of the number of rings (Fig. 4) seems to be dominated by the helicity of the inner radius, with a maximum at 8.

The fact that similar trends characterize geometrical chirality, enantioselectivity and optical rotation as functions of the number of rings, points to a possibility of correlating chromatographic column enantioselectivity towards the helicenes and optical rotation with quantitative chirality. The results are shown in Figs. 6 and 7. Note that this type of correlation distils the chirality factor and removes the size factor. Indeed, Fig. 6 does not follow the size strictly, but an order of points which, from left to right, is [6]-, [7]-, [10]-, [11]-, [9]-, [8]-, [13]-, and [14]-helicene

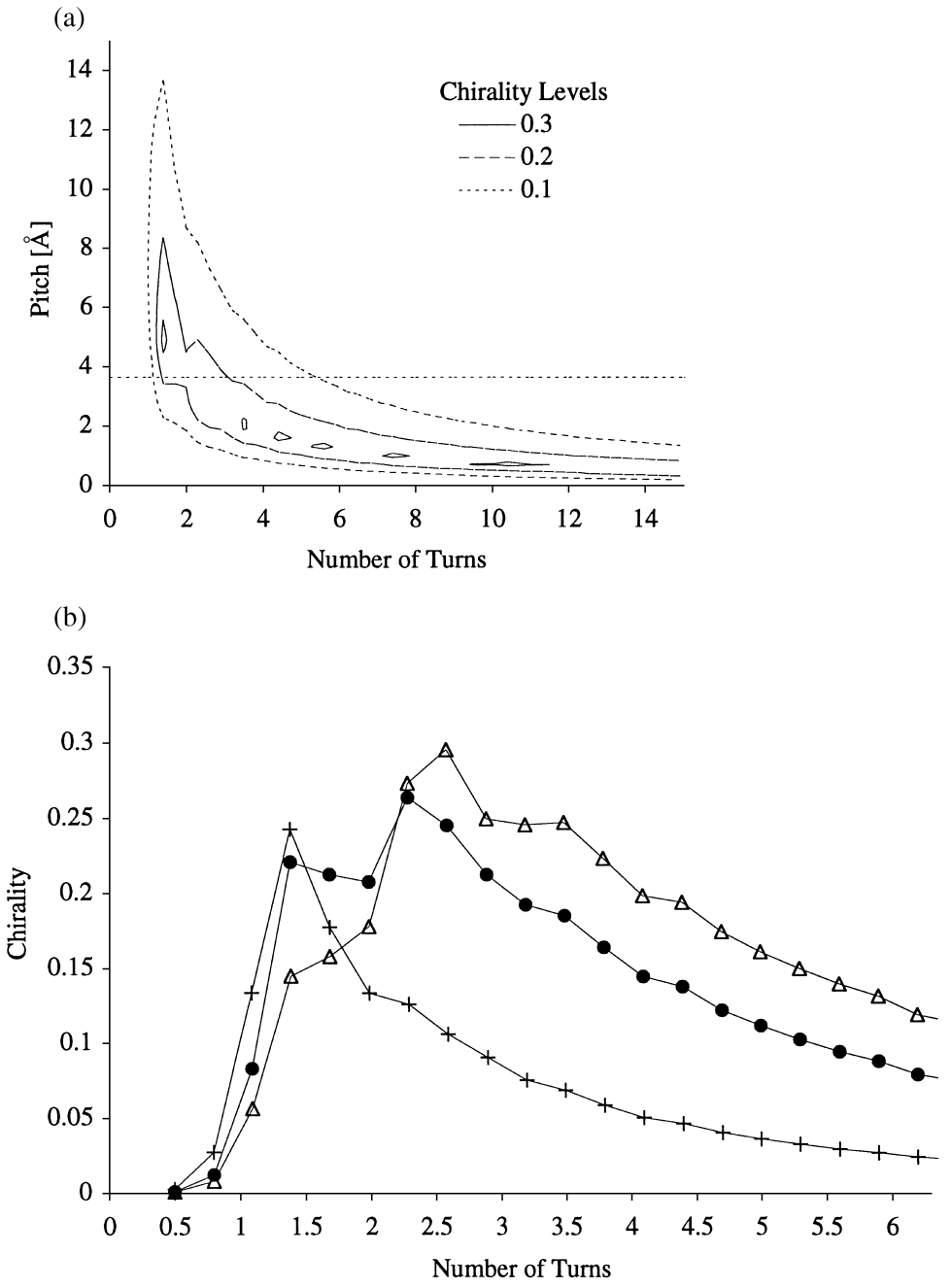


Figure 5. (a) The map of chirality of a helix ($r=2.9$ Å, $d=30$) as a function of the number of turns and of the pitch; (b) the chirality of helices (having helicene-like parameters ($p=3.64$ Å (an average helicene value), $d=30$ and (see Fig. 1b) $r=3.75$ Å (Δ), 2.9 Å (●)—see also cross-section in (a)—and 1.5 Å (+))) as a function of the number of turns

and Fig. 7 shows a similar trend. (Interestingly, diphenanthro[4,3-*a*;3′4′-*o*]picene,[10] which does not belong to the homologous series but has the shape of a double helicene, fits the general enantioselectivity trend of the regular helicenes (Fig. 6), indicating the importance of chirality as such.)

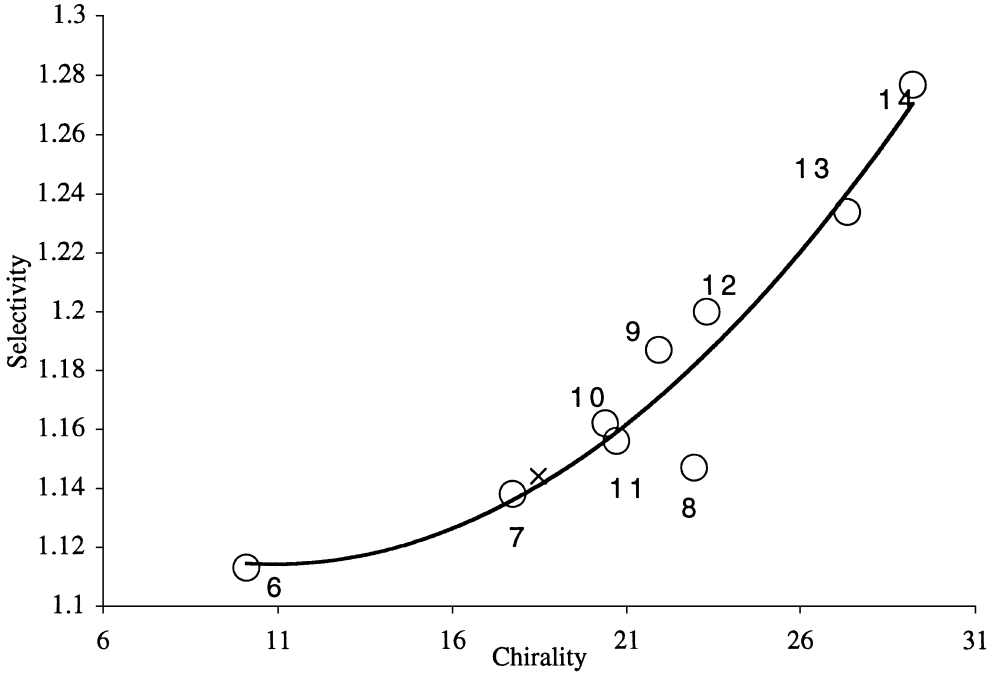


Figure 6. Chromatographic enantioselectivity as a function of the degree of chirality of the helicenes. Also shown (x) is a double helicene, diphenanthro[4,3-*a*;3′,4′-*o*]picene

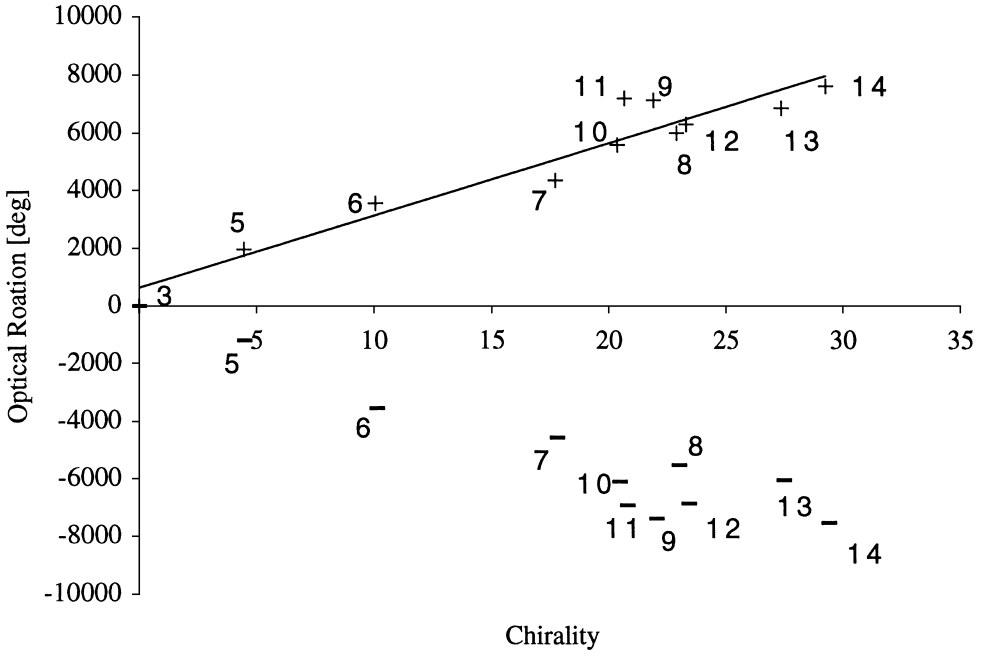


Figure 7. Optical rotation versus chirality. (–) M, (+) P

Two additional interesting correlations have been revealed as well. The first is with racemization energy. The analysis of correlations between the degree of chirality and the energetic barrier for enantiomerization was already the topic of a detailed study of chiral fullerenes.[3a] It was found there that the Stone–Wales enantiomerization is characterized by an approximately linear correlation between π-energy and the chirality content of the molecule; and that sensitivity to chirality changes, increases with size. Interestingly, this behavior is also observed for the different family of molecules analyzed here, the helicenes. Fig. 8 shows the measured[16] racemization activation energies versus chirality for the [5]–[9]-helicene series. An increase with chirality is observed, and again, with a hint for passing through a maximum (at [8]-helicene; enthalpies of racemizations[16] show the same trend).

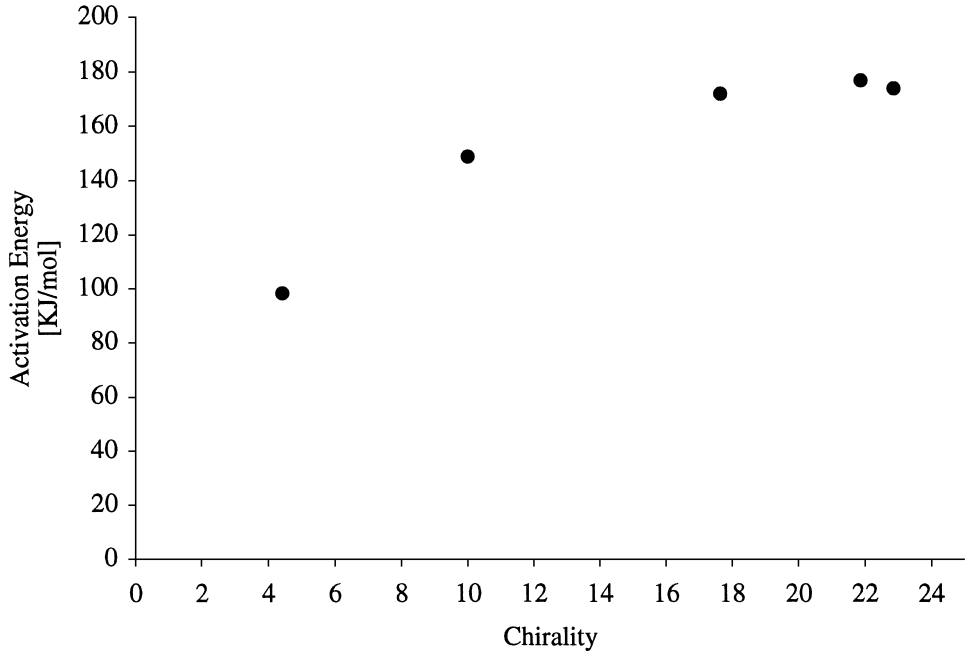


Figure 8. The activation energy of racemization as a function chirality for the [5]–[9]-helicenes (from left to right)

Our final parameter follows the pioneering investigations of Kitaigorodskii[17] on the relationship between shape and packing in the crystal, for which melting points are an indirect parameter, especially for homologous series. We found a good correlation between the melting points[18] and the chirality for a homochiral group of helicenes (Fig. 9). Significant in this correlation is the fact that extrapolation to $S(\sigma)=0$, phenanthrene, gives a melting point of 118°C, not very far from the experimental 101°C.

In conclusion, quantitative chirality provides a new angle of analysis of its effects. Since the chirality measure is a global shape parameter, one should search for quantitative chirality/property correlations mainly within homologous series for which the chemical properties are similar. Indeed, this approach proved useful for the family of the helicenes analysed here, in unveiling its quantitative geometric and functional chirality behavior and in explaining the trends found in Gil-Av's pioneering observations.[10,12]

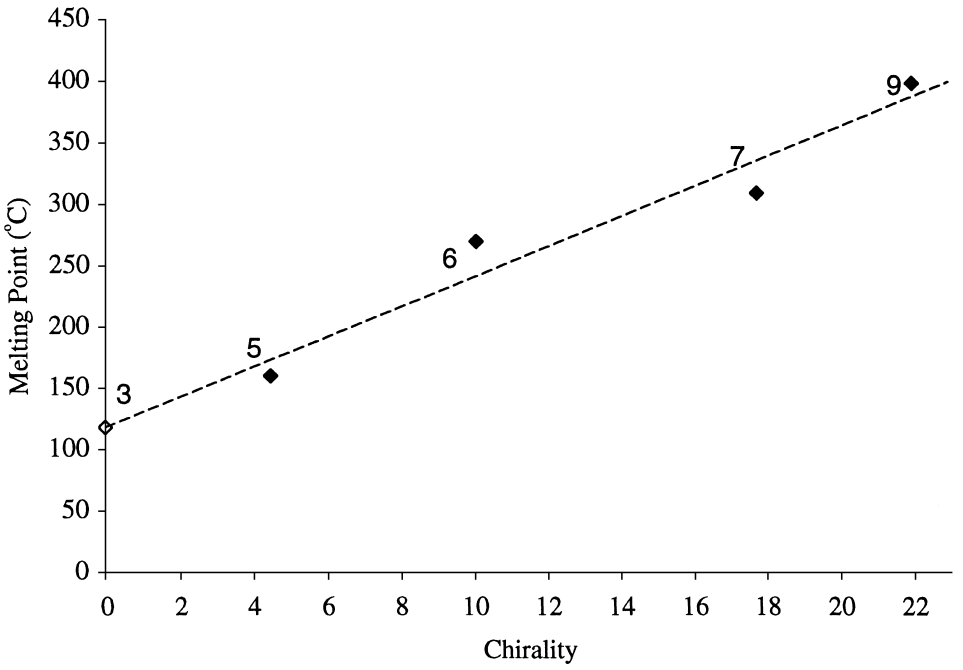


Figure 9. Melting points of single enantiomer helicene crystals as a function of chirality

## Acknowledgements

Supported by the US–Israel Binational Science Foundation, and by the Horowitz Foundation. We thank Professor Menachem Kaftori for help with the X-ray coordinates of the helicenes.

## References

1. Zabrodsky, H.; Avnir, D. *J. Am. Chem. Soc.* **1995**, *117*, 462.
2. (a) Pinto, Y.; Salomon, Y.; Avnir, D. *J. Math. Chem.* **1998**, *23*, 13; (b) Salomon, Y.; Avnir, D. *J. Comput. Chem.* **1999**, *20*, 772.
3. (a) Pinto, Y.; Fowler, P. W.; Mitchell, D.; Avnir, D. *J. Phys. Chem.* **1998**, *102*, 5776; (b) Keinan, S.; David, A. *J. Am. Chem. Soc.* **1998**, *120*, 6152; (c) Pinto, Y.; Hel-Ol, H. Z.; Avnir, D. *J. Chem. Soc., Faraday Trans.* **1996**, *92*, 2523.
4. (a) Zabrodsky, H.; Peleg, S.; Avnir, D. *J. Am. Chem. Soc.* **1992**, *114*, 7843; (b) Salomon, Y.; Avnir, D. *J. Comput. Chem.* **1999**, *20*, 772; (c) Katzenelson, O.; Zabrodsky, H.; Avnir, D. *Chem. Europ. J.* **1996**, *2*, 174.
5. (a) Avnir, D.; Katzenelson, O.; Keinan, S.; Pinsky, M.; Pinto, Y.; Salomon, Y.; Zabrodsky Hel-Or, H. In *Concepts in Chemistry*; Research Studies Press, Somerset, 1997; Chapter 9, pp. 283; (b) Avnir, D.; Zabrodsky Hel-Or, H.; Mezey, P. G. In *Encyclopedia of Computational Chemistry*; Wiley: Chichester, 1981; Vol. 4, p. 2890.
6. (a) Grimme, S. *Chem. Phys. Lett.* **1998**, *297*, 15; (b) Gao, D.; Schefzick, S.; Lipkowitz, K. B. *J. Am. Chem. Soc.* **1999**, *121*, 9481; (c) Lipkowitz, K. B.; Gao, D.; Katzenelson, O. *J. Am. Chem. Soc.* **1999**, *121*, 5559; (d) Alikhanidi, S.; Kuz'min, V. *J. Mol. Model.* **1999**, *5*, 116.
7. (a) Gilat, G. *Chem. Phys. Lett.* **1985**, *121*, 9; (b) Osipov, M. A.; Pickup, B. T.; Fehervari, M.; Dunmur, D. A. *Molec. Phys.* **1998**, *94*, 283; (c) Petitjean, M. *J. Math. Chem.* **1997**, *22*, 185; (d) Mezey, P. Z. *Chirality* **1998**, *10*, 173; (e) Mezey, P. G. *J. Math. Chem.* **1998**, *23*, 65; (f) and other references cited in these papers and in our reviews (Ref. 5).
8. Zabrodsky, H.; Peleg, S.; Avnir, D. *J. Am. Chem. Soc.* **1993**, *115*, 8278.

9. Munoz, V.; Serrano, L. *Nature: Struct. Biol.* **1994**, *1*, 399.
10. Gil-Av, E.; Mikes, F.; Boshart, G. *J. Chromatogr.* **1976**, *122*, 205.
11. The [5]-helicene was resolved as well but on a different coating, and therefore is not included here.
12. Gil-Av, E.; Mikes, F.; Boshart, G. *J. C. Chem. Comm.* **1976**, 99.
13. (a) Petricek, V.; Cisarova, I.; Hummel, L.; Kroupa, J.; Brezina, B. *Acta. Crystallogr., Sect. B. (Str. Sci.)* **1990**, *46*, 830; (b) Hirshfeld, F. L.; Sandler, S.; Scmidt, G. M. J. *J. Chem. Soc.* **1963**, 2108; (c) Kuroda, R. *J. Chem. Soc., Perkin Trans. 2* **1982**, 789; (d) Rango; Tsoucaris, G.; Declercq, J. P.; Germain, G.; Putzyes, J. P. *Cryst. Struct. Comm.* **1973**, *2*, 189; (e) Joly, M.; Defay, N.; Martin, R. H.; Declarcq, J. P.; Germain, G.; Soubrier-Payen, B.; Meerssche, M. v. *Helv. Chim. Acta.* **1977**, *60*, 537; (f) Bas, G. L.; Navaza, A.; Mauguen, d. R. C. Y. *Cryst. Struct. Comm.* **1976**, *5*, 357; (g) Bas, G. L.; Navaza, A.; Knossow, d. R. C. M. *Cryst. Struct. Comm.* **1976**, *5*, 713.
14. SPARTAN; 4.1 ed.; Wavefunction, Inc. 18401 Von Karman Ave., Ste. 370 Irvine, CA 96216, USA.
15. $C_2$-Symmetric helices are interesting from the point of view that they have two equidistant nearest achiral objects. These are two planes, representing two possible permutations. One is the permutation of each point with its $C_2$-symmetric counter point, and the other is the permutation of each point with itself. See Ref. 8 for technical details.
16. (a) [5]-Helicene: Martin R. H.; Marchant, M. J. *Tetrahedron Lett.* **1972**, 3707; (b) [6,7,8,9]-helicenes: Martin R. H.; Marchant, M. J. *Tetrahedron* **1974**, *30*, 347.
17. Kitaigorodskii, A. I. In *Organic Chemical Crystallography*; Consultants Bureau: New York, 1961; Chapter 4.
18. The melting points for [4]–[13]-helicenes are from *CRC Handbook of Chemistry and Physics*, Lide, D. R. Ed.-in-Chief, 72nd Edition, CRC Press: Boca Raton, 1991–1992; and for phenanthrene from the *Dictionary of Organic Compounds*, Cadogan, J. I. G., Ed.; 6th ed., Vol. 4, Chapman & Hall: London, 1996.